Finite Element Analysis of Human Joints
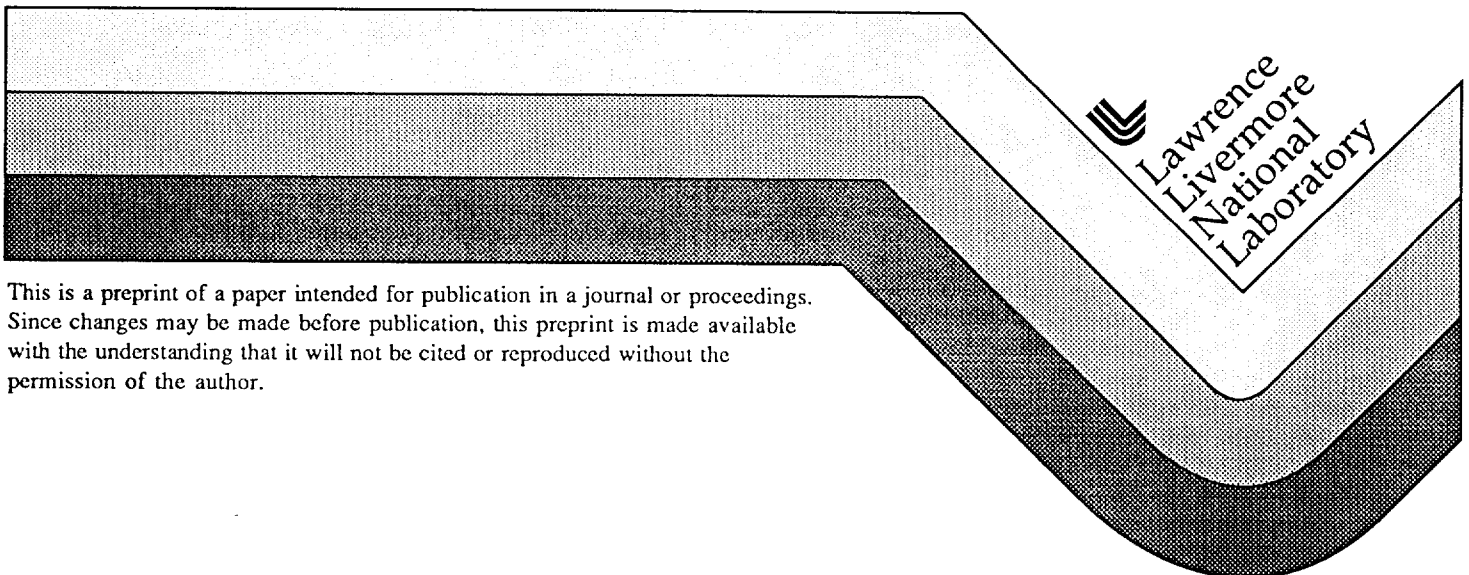
P-L. Bossart
and
K. Hollerbach
Lawrence Livermore National Laboratory
Livermore, California

September 1996

Finite element analysis of human joints

P-L. Bossart and K. Hollerbach
Lawrence Livermore National Laboratory

Abstract

Our work focuses on the development of finite element models (FEMs) that describe the biomechanics of human joints. Finite element modeling is becoming a standard tool in industrial applications. In highly complex problems such as those found in biomechanics research, however, the full potential of FEMs is just beginning to be explored, due to the absence of precise, high resolution medical data and the difficulties encountered in converting these enormous datasets into a form that is usable in FEMs. With increasing computing speed and memory available, it is now feasible to address these challenges. We address the first by acquiring data with a high resolution X-ray CT scanner and the latter by developing a semi-automated method for generating the volumetric meshes used in the FEM. Issues related to tomographic reconstruction, volume segmentation, the use of extracted surfaces to generate volumetric hexahedral meshes, and applications of the FEM are described.

Keywords : Computed tomography – volume segmentation – surface extraction – grid generation – finite elements – biomechanics – human joints

1 Introduction

This paper describes progress in developing FEMs of human joints. We aim to provide the tools for modeling the structural dynamics of joints, based on high resolution X-ray CT data, hexahedral volumetric meshes, material models for biological tissues, and physiologically appropriate boundary conditions. Even though FEM is becoming a standard tool in industry and has also gained acceptance as a tool to model the mechanics of individual biological tissues, it is just beginning to be used in whole joint biomechanics, because of the complexity of the joint systems being modeled. In order to be useful to the clinician and to the biomechanics researcher, FEM tools need to provide high quality results rapidly. Two main issues are run time and development time. We focus here on development time, which can be minimized by automating as much of the data processing as possible. In the model, the data are generated and used in the following progression: data acquisition (e.g., CT or other scanning modalities), segmentation, surface extraction, volumetric mesh generation, finite element modeling, visualization of results (Figure 1). Each of these steps, when completed fully manually, is time consuming (and frequently inaccurate). The research presented here increases model quality and decreases development time.

Motivation for this research lies in the areas of computational medicine and biology as well as in computer science: Future generations of the types of tools developed here will be useful in clinical diagnosis and treatment planning and evaluation, and in modeling general orthopedic systems. A number of other researchers share our general objectives in pursuing these research goals [1–3].

This work stems from a collaboration between several groups at LLNL. All high-resolution X-ray scanners, image processing and FEM software are available on-site. Thus, rather than optimizing each step of the dataflow independently from the others, we can adjust the techniques used and their results in order to optimize the dataflow as a whole.

2 X-ray CT and image processing

Typically, scanners used in the medical field have a spatial resolution of up to 1 mm, which is not acceptable for a precise definition of articular surfaces. Thus, an amputated hand was scanned with one of the industrial scanners that have been designed and constructed at the LLNL. The PCAT scanner was used, which can be reconfigured to handle objects of various sizes and attenuations [4]. The pixel size of the PCAT scanner is 150 μm, and is equal to the distance between CT slice planes. Thus, PCAT makes it possible to acquire high-spatial resolution isotropic volume elements (voxels). PCAT uses a 450 kVp X-ray source and a scintillating screen lens coupled to a 14-bit camera. This 2D detector helps acquire 720 projections (2.5 Gigabytes) rapidly. The reconstruction step is the most computationally-intensive and is performed using a parallelized Convolution Back-Projection (CBP) algorithm on a Silicon Graphics Onyx graphics hardware [5]. This fan-beam approximation to a cone-beam geometry only holds since the field of view was limited to a half-cone angle of 2 degrees. Future experiments will use a cone-beam reconstruction algorithm and a larger magnification ratio.

Several experiments were performed in order to assess the effects of data preprocessing and volume reconstruction. Removing the bad pixels that appear when a photon hits the CCD directly made the segmentation significantly easier. The correction for beam-hardening also proved extremely useful from the segmentation point of view. Several experiments were performed in order to choose the "best" cut-off frequency.

Segmentation is made difficult by the inhomogeneous trabecular structure of the bones (Figure 2). Choosing a threshold in a robust way is almost impossible, since the initial histogram is unimodal. Similarly, edge detectors produce a large number of spurious edges. Our approach relies on a simple model of the bone attenuation profiles. A 3D gray-scale morphological reconstruction [6] removes the texture and fills in the bones. The histogram becomes bimodal, and markers can then be extracted. This coarse segmentation is improved by computing the watershed lines [7], which are by construction located on gradient peaks and hence on sharp boundaries. These morphological operators rely on ordered queues, which help speed-up segmentation time dramatically.

Our attenuation model and the morphological approach were satisfactory in most cases. However, human interaction will always be needed to correct the coarse segmentation or the end-result. This kind of interaction requires computational tools that allow the user to visualize large data sets, manipulate the colormap to display false colors, perform interactive thresholding, overlay the segmentation mask, and save the corrected results.

Polygonal surfaces were extracted using both a contour based

approach [8] and a 3D approach [9], which performed well in our application, even in the case of branching or merging structures, while requiring no interaction or choice of parameters. However, the number of vertices required to represent a complex geometry is on the order of several millions. A decimation of the polygonal surface using the Decimate package [10] helped remove approximately 70% of the vertices, by replacing small triangles in flat regions by larger ones.

3 Volumetric mesh generation and finite element modeling

Most papers on automatic mesh generation focus on volumetric tetrahedral meshes. The algorithms used generally rely on a subdivision algorithm of the volume, such as in the octree approach. A mesh is then built by triangulating each of the cells of the volume. Changing slightly the coordinates of the vertices helps smooth the mesh and improve its quality. However, tetrahedral meshes are not suited for the dynamic simulations required in our applications. Structural engineers prefer hexahedral meshes, which help speed up the convergence of the numerical algorithms. However, automated hexahedral meshing is more challenging than automated tetrahedral meshing, since the global topology must be taken into consideration from the start.

In the development of an FEM of the hand, a template based approach to hexahedral, volumetric mesh generation has been developed and applied to the bones. Due to normal and sometimes pathological variations in anatomy, each person's finger bones are of a slightly different shape and size. However, since similarities usually outweigh differences, the problem of generating a mesh for each bone in all fingers of different people is greatly diminished by the development of one or more templates, each of which can be used to mesh more than one bone. In the method used to automate mesh generation, one template is chosen out of a library of templates, based on the geometry of the surface to be gridded, and then deformed to fit that geometry. A particular pre-defined (for the chosen template) sequence of steps to compute the volumetric grid is then performed.

Our work relies on the TrueGrid (XYZ Scientific Applications, Inc.) meshing package. The gridding algorithm begins with determining the long axis of the bone. (Each bone may exist in an arbitrary orientation in space.) Along that axis, a series of centroids is calculated, where each centroid lies in a plane perpendicular to the axis. The centroids are then connected in a line that forms the "spine" of the long bone. A number of planes are cut through the bone, each plane perpendicular to the spine at the centroid. The cross section of the bone is evaluated in each plane, and an index of variation from plane to plane is determined. Higher indices of variation result in finer local meshing. The spine is copied multiple times, and each copy is translated radially. Finally, a set of radial planar surfaces is added; all radial surfaces meet at the spine. The outer edge of each surface is defined by the original surface grid. To form the actual volumetric mesh, the computational (originally block shaped) mesh is placed inside the bone, and its vertices and faces are projected in a multi-step process (Figure 3) in such a way that each vertex lies at the intersection of the perpendicular cut plane and the outer edge of the closest radial surface, and each face approximates the original surface grid. With all vertices and faces in place, the internal nodes are then arranged to optimize the grid quality. The final result obtained is a high quality mesh that is suitable for finite element modeling (Figure 3(d)). Diagnostic measures, such as orthogonality of the elements, may be applied to confirm the mesh quality. Finger movement about the joint axes, using the finite element code NIKE3D (LLNL), provides further evidence of meshing success.

The hand bone models that were extracted from the X-ray CT data are combined with models of soft tissue such as ligamentous and cartilagenous structures. Normal joint motion can be simulated and soft tissue stresses calculated using this whole joint modeling approach. Muscle models will be added to future versions of the FEMs.

4 Conclusion

The major goal of this work was to create accurate FEMs of human joints from 3D X-ray CT data sets and to minimize the amount of human interaction required. We described each of the steps of the dataflow, namely preprocessing and tomographic reconstruction, segmentation, surface extraction and template-based mesh generation. The tools thus created can now be applied to any scanned data set. As a result, patient specific models can be developed rapidly. Ultimately, users of the FEMs will include biomechanics researchers and clinicians. For example, the modeling tools can provide guidance to an orthopedic surgeon repairing a joint. In addition, prosthetic joint implant designs may be improved.

Acknowledgments

References

[1] M.S. Shephard et al. The versatility of automatic mesh generators based on tree structures and advanced geometric constructs. *Comm. Appl. Num. Math.*, 4:379–392, 1988.

[2] J.A. Weiss et al. Finite element mesh generation of the knee and its soft tissues from CT data. In *Proceedings 2nd World Congress of Biomechanics (Amsterdam)*, 1994.

[3] K. Hollerbach et al. Patient-specific modeling of joint function. In *Proceedings SuperComputing Conference (San Diego), UCRL-TB-116901 rev.1*, 1995.

[4] V. Savona et al. Characterization of static- and fatigue-loaded carbon composites by X-ray CT. In D.O. Thompson and D.E. Chimenti, editors, *Review of Progress in Quantitative Nondestructive Evaluation*. Plenum Press, New York, 1995.

[5] S.G. Azevedo et al. Tomographic image reconstruction and rendering with texture-mapping hardware. In *Proceedings Mathematical Methods in Medical Imaging III, San Diego, California*. SPIE, July 24-29 1994.

[6] L. Vincent. Morphological grayscale reconstruction in image analysis: Applications and efficient algorithms. *I.E.E.E. Transactions on Image Processing*, 2(2):176–201, April 1993.

[7] L. Vincent and P. Soille. Watersheds in digital spaces: An efficient algorithm based on immersion simulations. *I.E.E.E. Transactions on Pattern Analysis and Machine Intelligence*, 13(6):583–598, June 1991.

[8] B. Geiger. *Three-Dimensional Modeling of Human Organs and its Application to Diagnosis and Surgical Planning*. PhD thesis, Ecole des Mines de Paris, 1993.

[9] W.E. Lorensen and H.E. Cline. Marching Cubes: a high resolution surface extraction algorithm. *Computer Graphics*, 21(3):163–169, 1987.

[10] W.J. Schroeder et al. Decimation of large triangle meshes. *Computer Graphics (SIGGRAPH 92)*, 26(2):65–70, 1992.
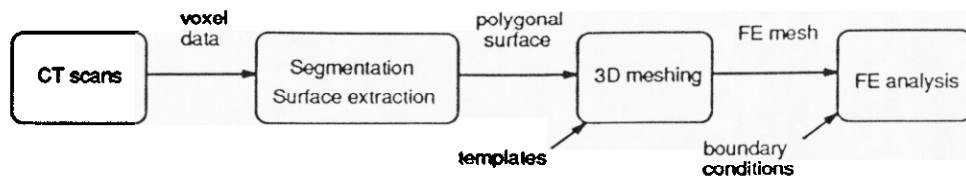
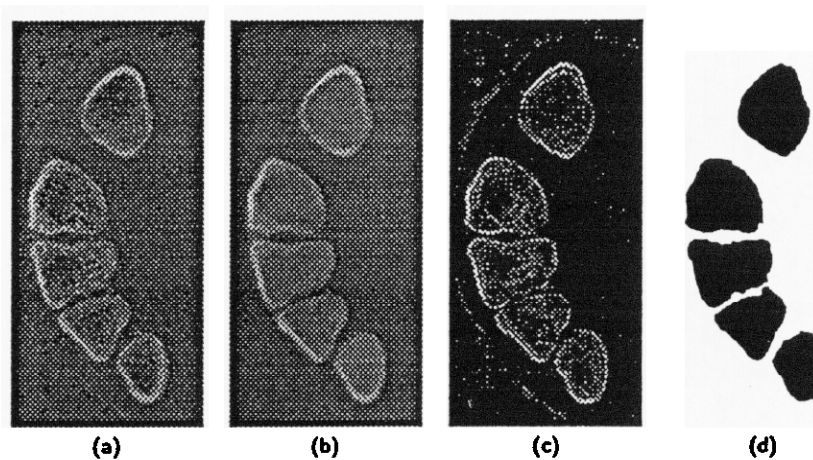Figure 1: General dataflow required to mesh 3D CT data sets.

Figure 2: Region-based segmentation using the watershed concept: (a) original image (b) result after gray-scale mathematical morphology image reconstruction; (c) gradient of the image in (a); (d) results of region-growing algorithm.
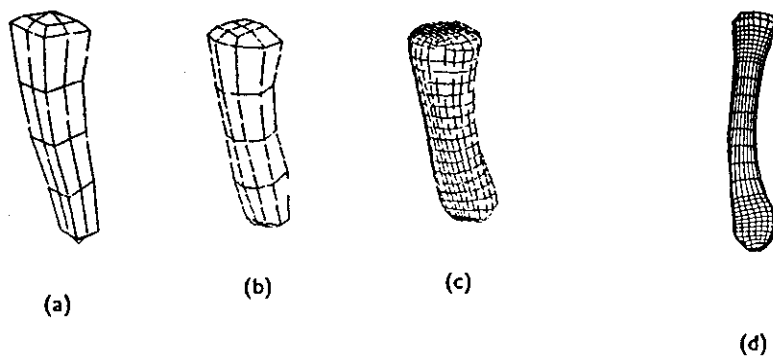

Figure 3: Overview of the grid generation for hand bones: (a) registration of the template with the extracted surface (b) projection onto the surface (c) interpolation and refinement (d) volumetric mesh of metacarpal bone extracted from 3D CT data